

We are IntechOpen, the world's leading publisher of Open Access books Built by scientists, for scientists

6,900

Open access books available

186,000

International authors and editors

200M

Downloads

Our authors are among the

154

Countries delivered to

TOP 1%

most cited scientists

12.2%

Contributors from top 500 universities



WEB OF SCIENCE™

Selection of our books indexed in the Book Citation Index
in Web of Science™ Core Collection (BKCI)

Interested in publishing with us?
Contact book.department@intechopen.com

Numbers displayed above are based on latest data collected.
For more information visit www.intechopen.com



Pyrolysis of Carbon-Doped ZnO Nanoparticles for Solar Cell Application

Luyolo Ntozakhe and Raymond Tichaona Taziwa

Abstract

It is very important to find new methods for improving the properties of nano-structured materials that can be used to replace the highly expensive and complicated techniques of fabricating ZnO nano-powders for solar cell applications. Pneumatic spray pyrolysis method offers a relatively inexpensive way of fabricating ZnO nanomaterials of controllable morphology, good crystallinity and uniform size distribution, which makes it a good candidate for the production of ZnO nanoparticles. Additionally, it has the advantage of producing ZnO NPs in one step directly on the substrate without the need for other wet chemistry processes like purification, drying and calcination. To that end, the present study emphasizes more on the design and optimization of spray pyrolysis system as well as on the pneumatic spray pyrolysis conditions for the production of carbon-doped ZnO nanoparticles. The un-doped and carbon-doped ZnO NPs were prepared using pneumatic spray pyrolysis employing zinc acetate as a precursor solution and tetrabutylammonium as a dopant. The fabricated un-doped and C-ZnO NPs were characterized for their morphological, structural and optical properties using SEMEDX, XRD and DRS. SEM analysis has revealed that the fabricated un-doped and C-ZnO NPs have spherical shape with mesoporous morphology. The cross-sectional SEM has also revealed that the film thickness changes with increasing dopant concentration from 0.31 to 0.41 μm at higher concentrations. Moreover, the EDX spectra have confirmed the presence of Zn and O atoms in the PSP-synthesized ZnO NPs. XRD analysis of both un-doped and C-ZnO has revealed the peaks belonging to hexagonal Wurtzite structure of ZnO. Additionally, the DRS has revealed a decrease in energy band gap of the synthesized ZnO NPs, with the increase in carbon dopant level.

Keywords: spray pyrolysis, zinc oxide, nanoparticle, pneumatic spray pyrolysis

1. Introduction

In recent decades, semiconducting metal oxide materials such as zinc oxide (ZnO), tin oxide (SnO_2), iron oxide (Fe_2O_3) and titanium dioxide (TiO_2) have become an area of research due to their great potential to solve environmental problems [1]. These wide-band-gap semiconductors are considered to have the ability to easily adjust the optoelectronic and transport properties of the metal oxide semiconductor material which makes them the promising candidates for several

applications such as gas sensing, photocatalysis, storage and solar energy conversion [2, 3]. Among them, zinc oxide is of special interest due to its wide range of properties such as direct band gap (3.37 eV at room temperature), non-toxicity, high photo stability and large exciton binding energy (60 meV) [3, 4]. Additionally, ZnO offers a low-cost material for solar cell electrodes, and its low price compared with other wide-band semiconductor nanomaterials makes it a good candidate for industrial applications.

Moreover, the physical and chemical properties of ZnO nanomaterial depend closely on the two geometrical parameters which are size and shape [5]. It can be easily processed into several nanostructures of different sizes, shape and morphologies such as nanorods, nanowires, nanonails, nanotubes, nanocombs, nanoflower, nanosheets, nanobelts, nanoparticles, etc. These nanostructures have become an area of interest for several applications due to their unique properties observed at nanoscale. Among the numerous nanostructures, nanoparticles (NPs) have attracted great attention in many device applications due to their unique catalytic, optical, magnetic and electrical properties because of their nanoscale dimensions [5, 6]. Particularly, the modified ZnO NPs have become function and integration of nanostructure assembly for dye-sensitized solar cells and nanoscale devices. The structural, morphological and optical properties of ZnO NPs can be improved and controlled by a chemical reaction which is a very crucial factor influencing the performance of semiconductor nanomaterials for many technological applications. Recently, great efforts have been made in the fabrication of doped ZnO nanomaterials in order to improve the morphological, structural and optical properties of nanomaterials specifically by modifying the surface properties such as electronic band gap, specific surface area, oxygen vacancies and crystal deficiencies [6, 7]. In previous articles, it has been reported that doping with non-metal elements such as C, S and N can improve the structural, morphological and vibrational properties of ZnO [7–9]. Doping with non-metal elements such as N or C has been reported to reduce the band gap of a wide-band semiconductor by enhancing a number of properties but not limited to ferromagnetism, magnets to transport properties and p-type conduction properties [8, 9].

There are several methods that have been used for the preparation of ZnO NPs which include physical methods and wet chemistry to solid-phase systems. However, the physical and chemical methods such as evaporation plasma [10], anodization [11, 12], spin on methods [13, 14], sputtering [15], ion-assisted deposition [16], reactive ion plating [17], laser ablation [18], filtered arc deposition [19] and atomic layer epitaxy [20] employed for the preparation of ZnO NPs in previous articles have been reported to require very expensive equipments, complex process controls and stringent reaction conditions. Additionally, these methods are responsible for the host of many problems such as generation of hazardous by-products, the use of toxic and flammable solvents, difficult controlling of morphology, very substrate dependent and require high vacuum temperature. The solid-based methods are the promising alternatives for the preparation of ZnO NPs due to their simplicity and high yield [9, 21]. Additionally, they do not require several steps like wet chemistry methods such as purification, calcinations, drying and extraction of material before use.

Moreover the solid-based techniques present no reagent concentration drawback as compared to other physical and chemical systems, which makes them more desirable for industrial scaling. Among the solid-based methods like laser ablation [21], sputtering coating [22], frequency electron tube sputtering (RFMS) [23], spin coating [24], aerosol-assisted chemical vapor deposition [25] and spray pyrolysis [26]. Spray pyrolysis (SP) offers a modest and cost-effective way of fabricating a number of nanostructures unlike many other film deposition techniques [27].

Moreover, SP has the potential to produce nanoparticles with consistent structural, optical and morphological properties in a one-step process without a need for other wet chemistry steps such as cleansing or excessive drying that contributes on the overall cost of fabrication of ZnO nanostructures [27, 28]. Additionally, this method is responsible to coat huge substrates and also offers the possibility for industrial scaling. Furthermore, SP process makes it possible to grow nanoparticles directly on the substrate and can be used directly as photo-anodes in the dye-sensitized solar cell device which in turn lowers the overall production cost of a solar cell device. The present study focuses on the novel pyrolysis of carbon-doped ZnO nanoparticles for solar cell application. Additionally, the death of scientific articles that report on the influence of carbon doping on ZnO NPs fabricated by PSP method was also the major motivation of the present compilation.

2. Design consideration of a pneumatic spray pyrolysis system

2.1 Experimental section

ZnO nanoparticles were prepared by spray pyrolysis technique employing zinc acetate ($\text{Zn}(\text{O}_2\text{CH}_3)_2$, Merck), ethanol (99.99% Sigma Aldrich), acetic acid (CH_3COOH) and tetrabutylammonium bromide (TBA) ($\text{C}_{16}\text{H}_{36}\text{BrN}$) as the starting materials. In typical experimental procedure, 0.1 M of zinc acetate was prepared by dissolving 5.4923 g $\text{Zn}(\text{O}_2\text{CH}_3)_2$ to a 250-ml volumetric flask containing minimum amount of ethanol, which results to the formation of zinc ethoxide solution. Then few drops of acetic acid were added to the zinc ethoxide ($\text{Zn}(\text{O}_2\text{CH}_3)_2$) solution as a stabilizer. The zinc ethoxide solution was sonicated inside the ultrasonicator for 30 min at 40°C. Tetrabutylammonium bromide about 1.55 ml was added to the resulting colorless solution of $\text{Zn}(\text{O}_2\text{CH}_3)_2$ in the volumetric flask. The 250-ml volumetric flask containing $\text{Zn}(\text{O}_2\text{CH}_3)_2$ and ($\text{C}_{16}\text{H}_{36}\text{BrN}$) was filled up to the mark with absolute ethanol. Several other carbon dopant ($\text{C}_{16}\text{H}_{36}\text{BrN}$) precursor solutions were prepared in much the same way as this one; the only difference was the volume of the dopant solution as shown in **Table 1**.

The precursor solution was then transferred into a chamber connected to a pneumatic pump prior to spray deposition. Firstly, the F:SnO₂ glass substrate was washed with detergent and then rinsed with distilled water, isopropanol, distilled water and acetone, followed by drying under hot air to evaporate the acetone. Then the fabrication of un-doped and C-ZnO NPs was done on well-dried F:SnO₂ glass substrate at a deposition temperature of 400°C. The fabricated NPs were then characterized using XRD spectra, obtained using a Bruker D8 Advance X-Ray diffractometer (XRD) with a Cu anode, generating K α radiation of wavelength 1.544 Å and operating at 40 kV and 40 mA, which was used to obtain the crystallographic phase and associated parameters of ZnO samples of the fabricated NPs. The XRD θ -2 θ patterns of ZnO NPs fabricated by PSP were recorded in the 2 θ range of

Sample #	Mass of zinc acetate (g)	Volume of TBA (ml)	Millimoles of TBA
Un-doped	5.4923	0	0
0.010 M	5.4925	1.55	2.51
0.015 M	5.4922	2.33	3.78
0.025 M	5.4924	3.88	6.30

Table 1.
Preparation of precursor of solutions.

30–100°C at room temperature. The elemental, structural and morphological properties of ZnO nanostructures were studied using field emission scanning electron microscope (FE-SEM) Zeiss Auriga SEM equipped with EDS with Smart SEM software at an accelerating voltage of 30 kV. High-resolution transmission electron microscope was used to determine the finer details relating to structural properties of un-doped and C-ZnO samples, obtained using a JEOL JEM 2100 HRTEM operating at 200 kV for high-resolution images with selected area electron diffraction (SAED) patterns. The confocal Raman imaging system (WITec GmbH, Ulm, Germany) alpha300RS was used to study the Raman active modes present in the ZnO samples. A fibre-coupled DPSS laser 532 nm with maximum output power after single-mode fibre coupling of 44 mW was used as the excitation source. Data were then collected using a multimode fibre into a high-throughput lens-based spectrograph (UHTS 300) with 300 mm focal length and two gratings 600 and 1800 g/mm, both blazed at 550 nm.

2.2 Experimental problems experienced with spray pyrolysis system at other laboratories for production of ZnO nanomaterials

This part outlines the practical knowledge or challenges that other authors experienced when operating spray pyrolysis (SP) technique. The knowledge collected from these authors was considered and played an imperative part in governing, assembling and monitoring the current spray pyrolysis (SP) system; hence we are also working with similar spray pyrolysis system. Additionally, the knowledge assembled assisted to shape several considerations in selecting the equipment such as furnace type, pneumatic pump size, reactor type, as well as type pneumatic vessel of the existing SP system. Lastly, the deposition conditions as well as material properties employed to enhance the design and development of the pneumatic spray pyrolysis system were also considered.

3. Experimental complications

3.1 Use of zinc acetate precursor solution

In this study, spray pyrolysis deposition was operated on the glass substrate lying perpendicular on the floor of aluminum tube inside the furnace. The zinc acetate was used as a precursor solution in this research. The spray pyrolysis system used in this research employed pneumatic pump which helps to blow the precursor solution to form mist of droplets inside the PSP vessel. There were few problems occurred with regards to formation of ZnO NPs such as the low solubility of zinc acetate salt in ethanol which needed to be heated up in order to dissolve completely in the solvent and the aluminum contaminations (impurities) initiated from the aluminum tube that was used as the reaction vessel. At higher temperatures, approximately 400°C and above, the aluminum tube impurities penetrate from the sample in the substrate holder which caused sample contamination. Hence, the fabricated ZnO nanoparticles were contaminated with aluminum. Due to aluminum impurities found in the fabricated ZnO NPs, there is a necessity to develop a tube reactor that can withstand deposition temperature of approximately 400°C and above, which does not introduce any impurity element in the fabricated nanomaterials. Similar problems were found in the literature in the case of TiO₂ nanoparticles where titanium tetrachloride was used as a precursor solution which generated massive complications with its chloride contaminants. It was observed that the cubic structures of sodium chloride crystallize fast and obstruct the

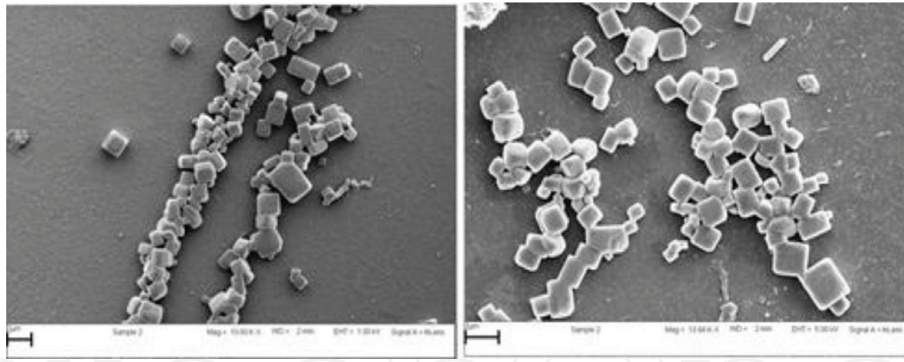


Figure 1.
SEM micrograph presenting the formation of NaCl crystals on top of the FTO glass substrate.

development of TiO₂ nanostructures on the uppermost of the glass substrates. Therefore, the contaminants of sodium initiated from the reactor tube that was used in the spray pyrolysis system. At higher temperature above 400°C, the sodium contaminant ions penetrate from the reactor tube which created nanomaterial impurities and reserved the development of TiO₂ nanomaterials on top of the glass substrates. **Figure 1** reveals the scanning electron microscopy image of cubic sodium chloride crystals on top of fluorine-doped tin oxide (FTO) glass substrates.

The zinc acetate precursor solution fumes are very toxic and acidic and have rapid diffusion rates at higher temperatures. The generated vapors were extremely acidic and portable at higher temperatures. Zinc acetate is known to be non-toxic, so these problems may be caused by the presence of acetic acid stabilizer in zinc acetate solution. The developed fumes produced almost rusted all the rubber tubing and seals fitted on the PSP system which may probably cause serious leakage problems in the system. Moreover the zinc acetate precursor vapors that are generated through deposition method have reserved the formation of zinc oxide nanoparticles; that is why it took us more hours to deposit a thin film of desirable thickness of 10 μm. This can also be probably due to low atomizer comprising the zinc acetate precursor capacities in the PSP vessel.

3.2 Substrate orientation

It was discovered that the thickness of the deposited ZnO thin film were not the same in all areas in the substrate, in some areas ZnO thin film had thicker layers compared to others and in some regions there were no ZnO NPs found completely as evidenced by **Figure 2**. It is noticed that only those regions of the substrates opposite the incoming vapor (aerosol) were completely covered. Then in other parts of the substrates such as those down the incoming vapor were moderately

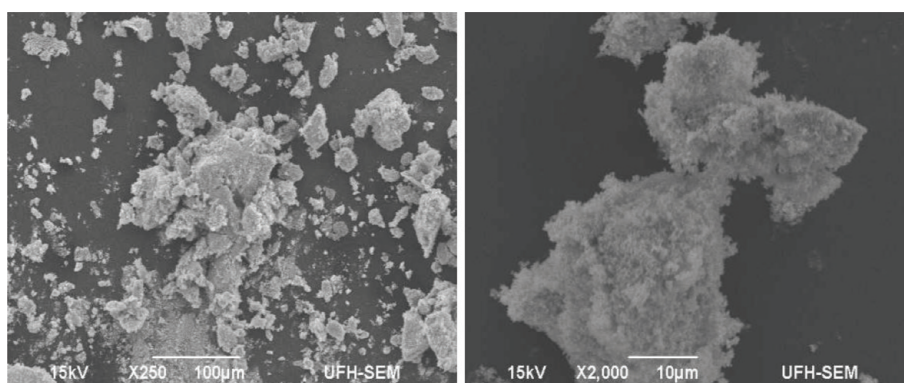


Figure 2.
SEM micrograph of non-uniformly coated ZnO thin film.

treated due to the position of the substrate (substrate orientation). The fabricated nanoparticles were found scattered in some areas of the substrates; this is probably due to poor substrate orientation or to unexpected temperature decrease when the furnace was turned off.

Moreover, the system took several hours to calm down to room temperature which made it difficult to run two or more samples a day, and the furnace used had poor heat insulation which dissipated heat into the working environment which made it very difficult to deposit thin films continuously. It was also discovered that the spray pyrolysis system has to cool down for more than 8 hours; otherwise, when quickly running a sample before 8 hours of cooling, the system just breaks down and it is very expensive to repair. Additionally, it was also noticed that after several hours of operation, the temperature rises up to beyond human comfort levels, which provided some difficulties in monitoring the spray pyrolysis deposition process continuously as the room temperature rises up to beyond 37°C. Hence it was very difficult to operate this kind of SP system right on a standard laboratory worktable because it presents a very high fire risk. Furthermore, all the rubber tubings could not resist the high temperatures and are needed to be changed regularly from time to time. This presented other possible health risks due to leakage of the evaporating zinc acetate precursor solution into the working atmosphere.

4. Pneumatic spray pyrolysis operation conditions

4.1 Safety

The pneumatic spray pyrolysis system needs to be closed at all times when running samples so it can strongly function on a normal laboratory workbench without any damage. The PSP system also needs to have an exhaust pipe into a suitably examined area to avoid exhaust of gas products into the work environment which are known to cause health problems in the long term. It has been reported that excessive inhalation of zinc acetate fumes causes nausea, diarrhea, metallic taste, kidney problem, stomach damage and vomiting. The tube furnace does not monitor the heat very well compared to split tube furnace so it was necessary to change the tube furnace by split tube furnace which can easily control the heat.

This has made it very simple and safe to work with aluminum tubing as the reaction reactor compared to quartz tubing. The split tube furnace was constructed in a manner that there is no heat that dissolute inside the work atmosphere. There was a necessity to use zinc acetate as a precursor solution since it is a safe, non-toxic liquid and can also prevent the requirement for high-priced gas handling method. Other precursor solutions like zinc chloride are not safe to use in the spray pyrolysis system because of the inherent problems of faster crystallization rate of chloride impurities which inhibits the formation of ZnO nanoparticles on the substrates. However, other salts like zinc nitrate and zinc naphthenate were other attractive electives for precursor materials for preparation of ZnO nanoparticle due to their safety, non-toxicity and their potential to produce well-adherent and uniform ZnO film.

4.2 Pneumatic spraying vessel

The main aim of this study was to design a pneumatic spray pyrolysis system that is capable of generating nanomaterials on a glass substrate, which can be compared to other previous findings by Mwakikunga et al. [29] and Taziwa et al. [30] using an ultrasonic reaction method consisting of an exciting capacity of 0.1 m³.

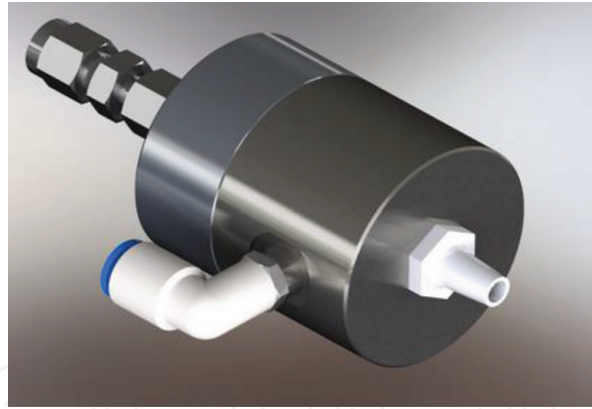


Figure 3.
Image of the PSP reaction vessel used in this study [31].

Figure 3 displays a PSP reaction vessel employed for fabrication of ZnO nanomaterials in this study. The precursor solution of zinc ethoxide is blown by the air from the pump to form a mist of droplets inside the PSP vessel. The material employed for the container presented a non-corrosive atmosphere for the accommodation of ZnO precursor solution.

4.3 Selection of ZnO precursor

The selection of a precursor solution became one of the most imperative methods in the fabrication of ZnO nanostructures using spray pyrolysis technique. The properties (physical and chemical) of the precursor solution are influenced by the solvent chosen, nature of salt, the salt concentration as well as other additive or extracts involved [32]. Hence, the structural, morphological and optical properties of the deposited thin films are easily formed through altering the nature of the precursor solution. The effects of preparation technique and zinc oxide precursor solutions like zinc nitrate and zinc chloride were studied. It has been reported that zinc chloride results in the formation of several unknown impurities in the sample which requires it to undergo various steps of wet chemistry such as washing, drying and calcination. Additionally, the samples originating from zinc chloride in the presence of sodium hydroxide as the precursor solution always produce the hexagonal Wurtzite structure of ZnO, while samples produced from the aqueous solution of zinc nitrate mostly result in the formation of polycrystalline structure of ZnO.

The preparation of ZnO using other methods of synthesis such as hydrolysis of zinc acetylacetonate monohydrate or hydrolysis of zinc naphthenate at room temperature also results in the formation of the hexagonal Wurtzite structure of ZnO. In the present study, the zinc acetate was chosen as the precursor of choice as the ZnO precursor. Despite the fact that it is one of the mostly used precursors in previous studies, it is a good candidate for solar cell production because the zinc acetate precursor can be easily modified with other additives like acetic acid as well as dopant to improve the resulting ZnO properties. Many published articles in the literature have highlighted that the morphologies of the fabricated nanostructures can be successfully modified by introducing preservatives into the precursor solutions [30]. Introduction of additives like CH_3COOH (acetic acid) in the precursor solution results in the alteration of the structure of the deposited ZnO films from fractured to a fractured free reticular. The change in the morphology of the deposited nanoparticles can be accredited to the change in precursor solution interaction. Hence in this work, zinc acetate was employed as the precursor for the fabrication of ZnO nanostructures. Moreover, the precursor consists of following advantages:

(1) non-corrosive and non-hazardous, recorded as a slight film, (2) extremely filtered and has nearly unlimited shelf life, (3) very unstable at slight temperatures such as 50°C, which indicates that it can be freely decomposed, (4) simply sprayed true without reduction, (5) it is relatively easy to handle as a liquid, even if it can be visible to an unmasked flame. The indication that it is not hazardous implies that presence of zinc acetate system is a relatively easy and safe task, as no special gas handling equipment is required, (6) it has been observed that it cannot be easily affected by the presence of oxygen in the atmosphere; hence there was no carrier gas used during the synthesis process.

4.4 Geometry mechanism

Another important aspect that required special consideration was the matter of substrate location and orientation in the reactor tube inside the furnace. It was almost impossible to deposit ZnO NPs at a position of 30° angle or with a substrate placed on the surface of the aluminum tube as this has been reported to cause inhomogeneous thin film coating. To avoid inhomogeneous thin film coating, there was a need to select or design an aluminum substrate holder that preserves the substrate at an angle of 90° so that it can directly interact with the incoming aerosol. The aluminum was selected as a metal of high quality since it presents several advantages such as its stability at deposition temperatures between 400 and 500°C, excellent conductor of heat and it allows preheating of the substrates before the deposition of thin film.

4.5 Deposition area

Almost all the types of solar cells have an active area where the semiconductor nanomaterials are deposited in the glass substrate and the rest of the area on the glass substrate can be utilized for solar cell contacts. Hence, it is necessary to mask the glass substrate in order to allow the formation of a thin film size of 0.5 cm² that is normally required for dye-sensitized solar cell application. Hence a substrate holder was designed in such a way that it could stand inside the aluminum tube reactor and at the same time other contact areas were masked during deposition.

4.6 Selection of spray reactor (split tube furnace)

There are several methods that can be used to synthesize the ZnO nanomaterials including wet chemistry techniques and solid-based methods. The solid-based methods are the most preferred for producing nanomaterials compared to solution-based methods due to their simplicity, high yield and they do not require several steps of wet chemistry such as washing, drying as well as calcination. The spray pyrolysis system that employ tubular reactor systems (furnace) offer several advantages such as (a) operation simplicity, (b) minimum throughput, (c) smaller current budget, (d) inexpensive to operate and (e) does not require successive heat treatment just after sample synthesis. Additionally, when tubular reactor is employed in spray pyrolysis method, each droplet holds the precursor in the exact the same stoichiometry as preferred in the product unlike in other reactors such as vapor flame reactor where the variety of the products is limited by the choice of metal precursors with enough vapor pressure to provide the preferred amount of the species into the reactor. Moreover, in spray pyrolysis reactor, the droplet basically serves as an isolated micro-reactor which is a vast advantage over the vapor phase method because



Figure 4.
Image of the split tube furnace and aluminum reactor used in the fabrication of ZnO nanostructures.

most reactants are expected to evaporate concurrently with extra precaution to achieve the preferred stoichiometry in vapor flame reactor. Furthermore, spray pyrolysis employing furnace reactor offers more quality at very less operational cost and least operative skill than flame reactors which have very high operating budgets, and the value of the resulting product in neither stoichiometry nor crystalline morphology leaves a proportion to be anticipated. The tubular furnace reactor that is used in the PSP offers a well-controlled temperature (heat) zone over prolonged period of time for conversion of the precursor to the required final product. In addition, tubular reactor method also provides the possibility for industrial scaling. Hence spray pyrolysis method is referred as a method that draws on the advantage of outstanding three-dimensional mixing of the reactants and was also established for multi component systems. These facts are generally one of the drivers of the high-quality tubular reactor used in this work as revealed here in **Figure 4**. **Figure 4** displays the split tube furnace and the aluminum tube that were employed in this study for the synthesis of ZnO NPs, respectively.

5. Pneumatic spray pyrolysis system

The spray pyrolysis system consists of a (i) split tube furnace, (ii) aluminum reactor as the reaction zone, (iii) nebulizer that converts the starting solution into droplets, (iv) sample holder (i.e. filter, electrostatic precipitator and thermophoretic sampler) and (v) an exhaust. The pneumatic spray pyrolysis (PSP) system was designed and assembled specifically for the fabrication of ZnO nanomaterials for solar cell applications. **Figure 5** displays the schematic diagram of the PSP technique system used in this study for the fabrication of ZnO nanostructures.

Pneumatic spray pyrolysis deposition involves forcing the precursor solution into fine nozzles to yield the mist of droplets of the precursor liquid at audible sound. The generated precursor droplets in a chamber are then transported into the furnace (heated zone) through the aluminum tube onto a preheated glass substrate. The PSP reaction was carried out at room temperature unlike in ultrasonic spray pyrolysis (USP) where the reaction is carried out in an oxygen-free environment using nitrogen or argon as a carrier gas to elude oxide formation and to declare reduction to metal that occurs in the high-temperature reaction zone. The spray

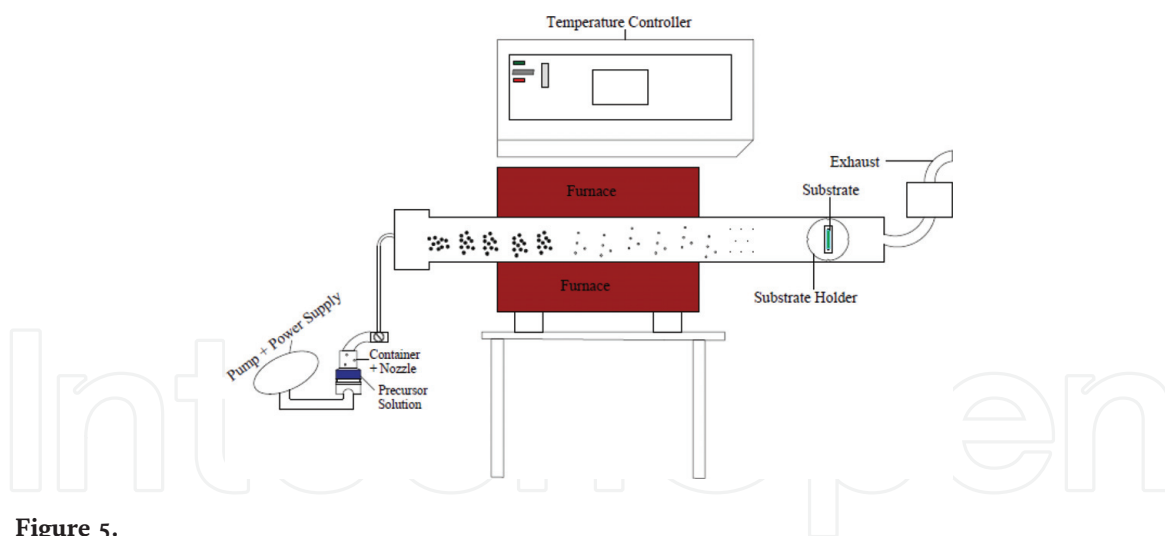


Figure 5.
Schematic diagram of the PSP system used for deposition of ZnO nanomaterials.

pyrolysis reaction was run at a constant flow rate that was automatically controlled by the pneumatic pump at an average flow rate of 5–6 ml/min. The spray pyrolysis deposition was accomplished at the system functioning at a temperature of 400°C; this is due to sufficient residence time consumed by spray vapor droplets inside the furnace. The deposition temperature and flow rate have the influence on the shape, size and the structure of the deposited thin film. The ZnO thin films were deposited on top of the fluorine-doped tin oxide (FTO) glass substrates.

5.1 Pneumatic spray pyrolysis mechanism for droplet generation

In order for the droplet to be generated, the precursor solution must have sufficient high velocity of ejection in the pneumatic vessel. The speed of the air from the pneumatic pump measures the droplet size in the pneumatic atomization. Hence increasing the pneumatic pump speed leads to the formation of very small droplets. The splitting of the precursor solution occurs to produce droplets and is transferred from the liquid pneumatic source interface to the surrounding air as a mist of very fine dense droplets. This process usually happens when the precursor solution is subjected to sufficiently high intensity of pneumatic field. Spraying of the liquid is done in the presence of very high pneumatic pump speed to the precursor solution which results in the formation of aerosols with constant droplet size and depends closely on the characteristics of the liquid. There are several main features which demonstrate scale pneumatic spray pyrolysis such as aerosol pneumatic generator, high temperature furnace with a fire wall heated reactor, electrostatic filter as well as the vacuum system. The precursor solution sheet can be interrupted to form droplets when the high-velocity air conveys its energy to the precursor. **Figure 6** shows the schematic diagram for the droplet generation at the crest of the waves.

Ultrafine droplets with good sphericity and uniform size distribution can be attained only if the energy of precursor sheet fragmentation can be delivered by the use of pneumatic energy [33]. The spray of very small ultra-fine droplets is properly produced by high pneumatic atomization speed. Traditional mechanical approaches such as pressure or gas-assisted methods are not considered to be advantageous on the generation of very small droplets compared to pneumatic atomization because it has some specific characteristics that make it more valuable [29, 34, 35]. Pneumatic atomization is a very productive method of generating small droplets. The ZnO nanostructures were formed after the precursor droplets have been generated.

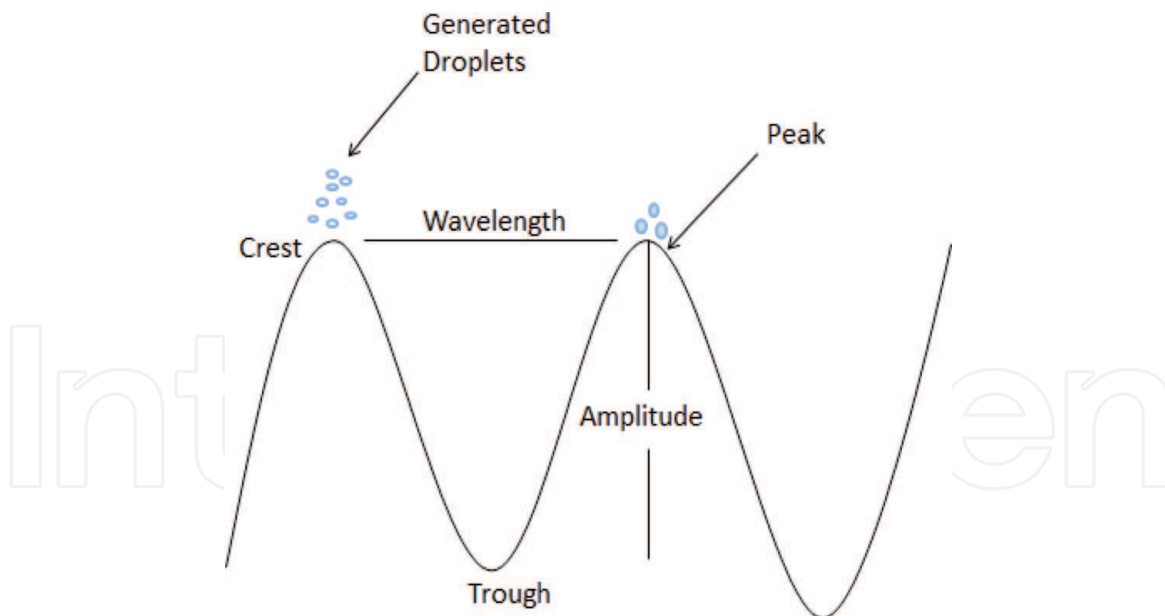


Figure 6.
Schematic presentation of droplet generation at the crest of capillary waves.

5.2 Pyrolysis of ZnO precursor solution

Generally, when a droplet hits the surface of the substrate, many processes take place simultaneously such as the vaporization of residual solvent, droplet diffusion as well as the corrosion of salt. Several design cores exist for the pyrolysis of the precursor depending upon the chemical environment. The mechanism of the reaction of zinc acetate aerosol for the formation of ZnO depends on the size of the droplet. The decomposition conditions are assumed to be similar to a CVD process if the majority of the aerosol is in gas phase when in contact with the substrate. The majority of aerosols with larger droplet sizes could not have enough time to vaporize completely, while those with small droplet sizes are easily decomposed by pyrolysis before reaching the substrate. Hence the droplet size distribution is small enough in the pneumatic spraying. At very low temperatures, the decomposition rate is assumed to be slower than the deposition rate which results in the formation of liquid film on the surface as revealed by process A in the above diagram. The resulting layer is slowly dried; however, it can still have several organics and possible cracks on it. At this stage a small amount of zinc oxide as a hydrated white precipitate will be present in its amorphous phase. **Figure 7** shows the deposition processes of the aerosol droplet transport that occur with rising the temperature of the substrate.

As the substrate temperature increases to higher temperatures in process B, the solvent from the precursor solution vaporizes completely through the trip of the droplet just before striking the floor (surface), and the precipitate hits the substrate where corrosion of the aerosol takes place [36]. As the temperatures increase in process C, the solvent also evaporates before the droplets strike the substrate, and the solid precipitate melts and sublimates which results in diffusion of the vapor to the substrate and commences a chemical reaction process. This is the stage where the adherent films can mostly be achieved by CVD [36, 37]. At higher temperatures in process D, the precursor solution evaporates just before hitting the glass substrate; at this stage the vapor phase first experiences a chemical reaction before invading on top of the substrate which results in the formation of solid nanoparticles that remain to the floor of the substrate. Hence we can speculate that the ZnO solid films can be yielded by evaporation and corrosion of the precursor prior to striking the substrate at high temperatures. Additionally, the existence of huge nanoparticles on the surface

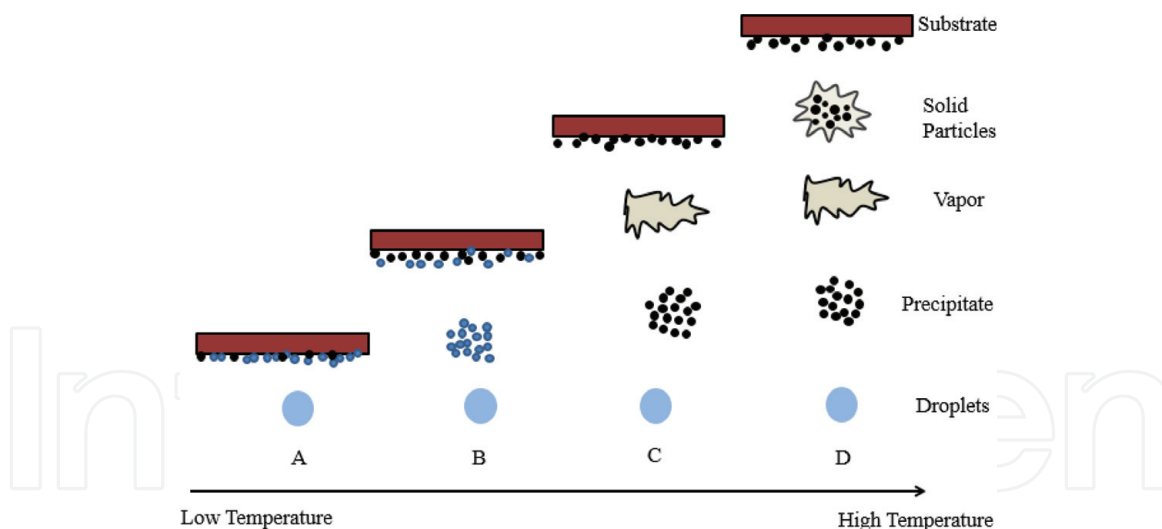
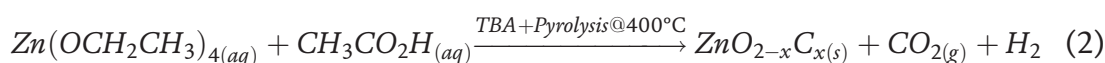
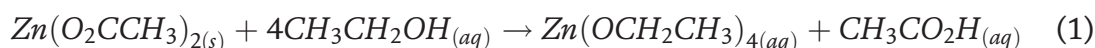


Figure 7.

Illustration of spray droplet transportation and deposition on the substrate at different temperatures.

of the substrate can be due to very large droplets, which are not completely decomposed when arrived at the substrate. The chemical reaction mechanism for the formation of ZnO nanoparticles is more similar to that proposed by Livage [35, 38] in the production of vanadium oxide NPs and similar to the one adopted by Taziwa et al. [29, 30] in the production of carbon-doped titanium dioxide NPs and is shown by the following reactions:



6. Operation of PSP system

Pneumatic spray pyrolysis can be used to generate an aerosol from a dilute aqueous salt solution (ZnO precursor solution), resulting in the formation of nanoparticles with a narrow size distribution. The reaction was carried at a constant flow rate and was automatically controlled by the pneumatic pump which was used to blow the precursor solution in the PSP vessel. The pneumatic spray deposition was performed at the system operating at an average flow rate of 5–6 ml/min at a temperature of 400°C; this is probably due to sufficient residence times consumed by spray vapor droplets into the furnace. **Table 2** reveals the typical deposition factors of the chosen precursor.

Process parameters	Pneumatic spray pyrolysis @400°C
PSP pump air flow rate	5–6 ml/min
PSP vessel pressure (atm)	1
Precursor temperature (°C)	25
Precursor pH	1.27
Substrate type and temperature (°C)	Glass/400°C
Deposition time (h)	4
Deposition angle (°)	90
Annealing temperature (°C)	400

Table 2.

Operational conditions for PSP method.

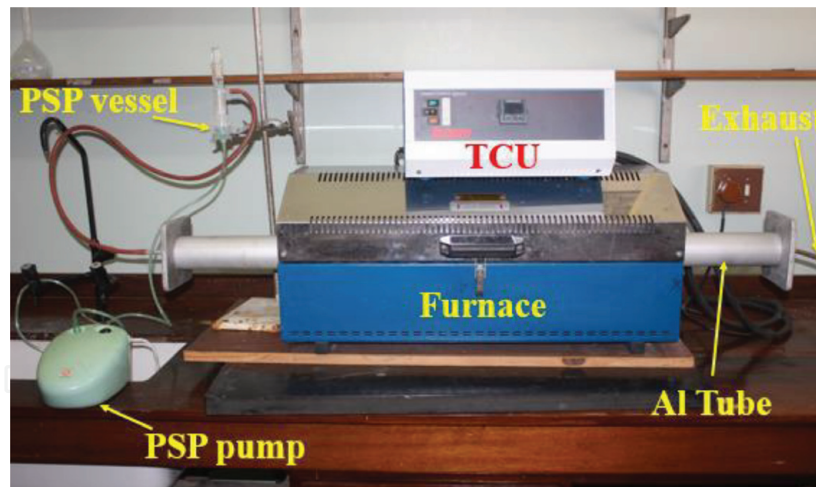


Figure 8.
Actual photograph of the horizontal pneumatic spray pyrolysis system utilized in the study in its final form.

- 1.** Prepare the desired precursor solution as outlined in table 2 above in a 250 ml volumetric flask
- 2.** Transfer the precursor solution into a Pneumatic spray pyrolysis vessel. Ensure that the PSP vessel is completely closed to avoid leakage of the precursor solution.
- 3.** Into an Aluminum tubing/quartz tubing insert the aluminum substrate holder housing the F: SnO₂ glass substrate. Set the furnace to the desired temperature. Allow it to stand for 10-15 minutes. Until the substrate has reached the furnace temperature
- 4.** Connect the inlet of the aluminum/quartz tubing to the outlet of the Pneumatic vessel and the outlet to the (1) exhaust for thin film synthesis and/or (2) to the nano powder collection system
- 5.** Switch on the PSP pump to the desired flow rate and then carry out spray deposition.
- 6.** To finish pneumatic spray deposition, simultaneously switch off the furnace and the PSP pump. Anneal the sample until they are ready for collection

Figure 9.
A schematic indicating the necessary steps to set up and perform pneumatic spray depositions for synthesis of pure ZnO and carbon-doped ZnO.

The pneumatic spray pyrolysis system in its final form is clearly revealed here in **Figure 8**; it is incorporated with all the other components as well as those listed in other sections above. In addition, the diagram in **Figure 9** highlights the necessary steps to set up and perform depositions of ZnO employing PSP system using a horizontal reactor. The aluminum substrate holder was employed in all conditions for ZnO thin film production.

7. Results and discussion

7.1 Scanning electron microscopy (SEM)

Figure 10 shows the SEM micrographs of the un-doped and C-ZnO NPs fabricated using the PSP system with different levels of carbon dopants. The SEM images of synthesized un-doped and C-ZnO samples have revealed the formation of spherical-shaped ZnO NPs with uneven grain size distribution. The SEM micrographs of the synthesized samples have revealed the change in morphology and shape of un-doped and C-ZnO NPs as the level of dopant increases. Additionally, the SEM images have revealed that the un-doped and C-ZnO samples consist of mesoporous morphology with a multiple porous network structure. Moreover, the introduction of carbon in the ZnO matrix has resulted in the formation of large spherical NPs surrounded by small NPs.

The inserts in **Figure 10** show an elemental analysis of the un-doped and C-ZnO NPs which was performed with energy dispersive X-ray (EDX) spectroscopy, using a scanning electron microscope (SEM). The EDX spectra of both un-doped and carbon-doped ZnO NPs revealed the existence of Zn, O and Al which indicates the successful pyrolysis of zinc ethoxide to form ZnO nanomaterials. Additionally, the presence of the C, Zn and O elements in the carbon-doped samples indicates the

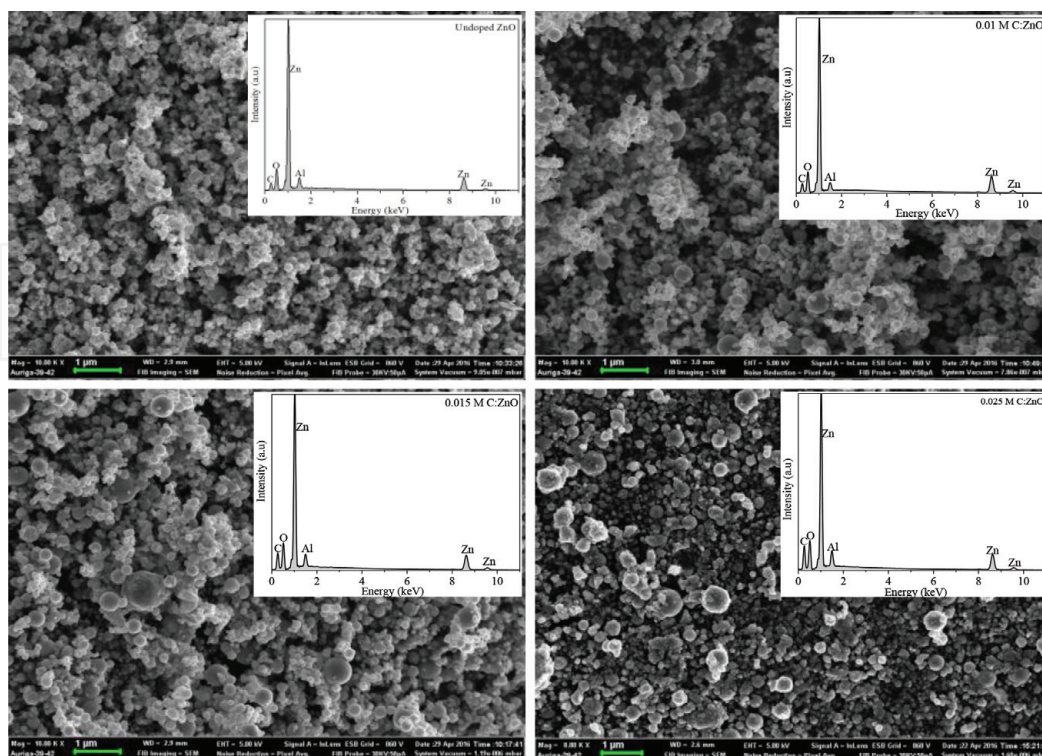


Figure 10. SEM micrographs of (a) un-doped ZnO, (b) 0.01 M C-ZnO, (c) 0.015 M C:ZnO and (d) 0.025 M C:ZnO samples. Moreover, inserts in (a), (b), (c) and (d) show typical EDX spectra of the synthesized un-doped and C-ZnO nanostructures.

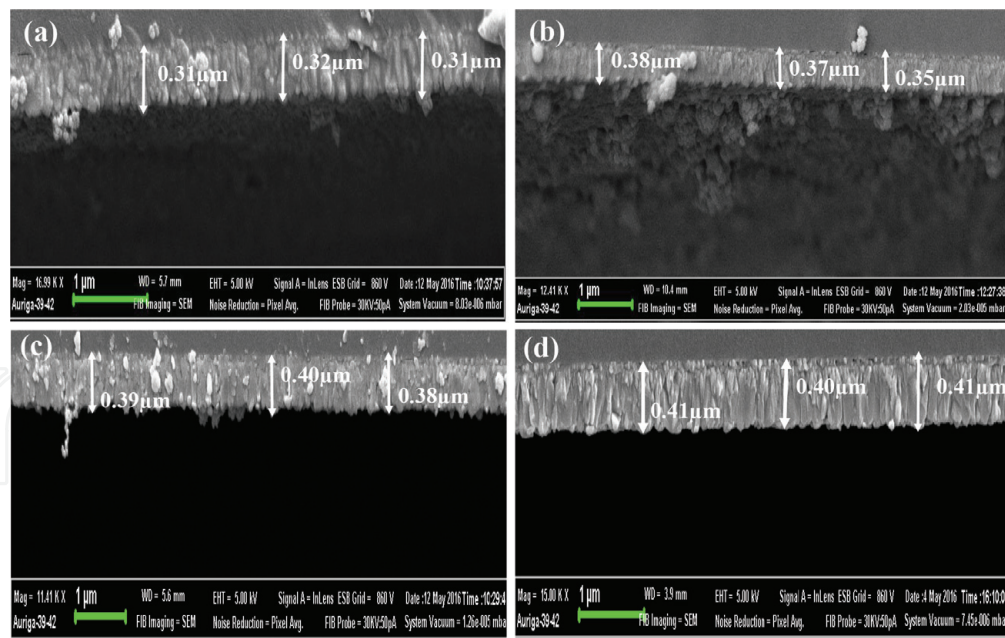


Figure 11. The cross-sectional SEM micrographs of (a) un-doped ZnO, (b) 0.01 M C-ZnO, (c) 0.015 M C:ZnO and (d) 0.025 M C:ZnO samples

effective modification of carbon in the ZnO matrix. Furthermore, the EDX spectra of the synthesized ZnO NPs have revealed the existence of Al in all the samples; this is due to the aluminum tube reactors and aluminum substrate holder used in the pneumatic spray pyrolysis system.

7.2 Cross-sectional SEM

Figure 11 shows cross-sectional SEM images of the un-doped and carbon-doped ZnO thin films deposited by pneumatic spray pyrolysis technique. The thickness of the thin films was measured using cross-sectional SEM method. It is observed that the film thickness changes with increasing dopant concentration from 0.31 to 0.41 μm . The thickness of the un-doped ZnO thin film is 3.1–3.2 which was gradually increased due to the presence of dopant to 0.3538 at lower concentrations of dopant and 0.38–0.41 at higher concentrations. This implies that the introduction of carbon to ZnO lattice also affects the film thickness of the fabricated ZnO NPs as evidenced by **Figure 11**.

7.3 X-ray diffraction

Figure 12 shows the X-ray diffraction patterns of the ZnO NPs fabricated by PSP technique and recorded in the 2θ range of $30\text{--}80^\circ$ at room temperature. The XRD patterns of both un-doped and C-ZnO samples have displayed the characteristic peaks of the hexagonal Wurtzite structure. The diffractograms obtained at room temperature for both un-doped and C-ZnO were observed by XRD lines at 31.90 , 34.50 , 36.34 , 47.73 , 56.88 , 63.04 , 68.20 and 77.33° . These lines are indexed as (100), (002), (101), (102), (110), (103), (200) and (112), respectively. The sharp and intense peaks for the dominant peak at 36.34° indexed (101) in the XRD diffractograms show that the synthesized samples are highly crystalline.

The effect of carbon doping on the ZnO lattice was cross-examined by monitoring the three dominant peak positions of (100), (002) and (001) planes. The introduction of carbon doping resulted in a peak shift to higher 2θ wave numbers,

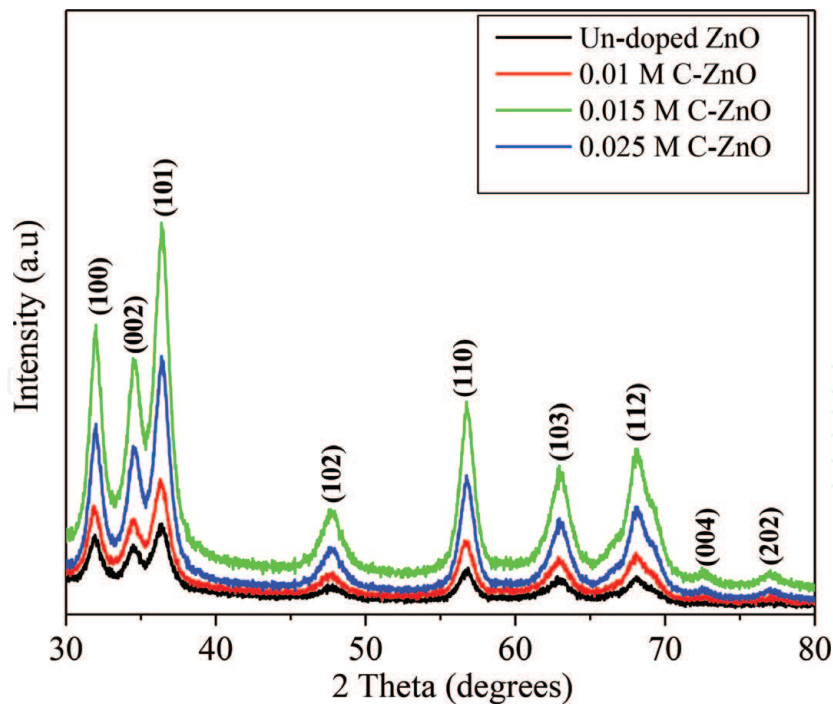


Figure 12.
XRD patterns of ZnO NPs synthesized by PSP technique.

which indicates substitutional doping in ZnO samples. In this work, the crystallite size was calculated using the Scherrer method which is considered as a standard method. The Scherrer method has revealed that the crystallite size increases as the dopant levels increase. The calculated crystallite sizes for both un-doped and C-ZnO were 9.60, 9.99, 0.96 and 10.22 nm for un-doped ZnO, 0.01 M C-ZnO, 0.015 M C: ZnO and 0.025 M C:ZnO samples, respectively.

7.4 Diffuse reflectance spectroscopy (DRS)

Figure 13 shows the UV-Vis diffuse reflectance spectra (DRS) of the synthesized un-doped and C-doped ZnO NPs. The UV-Vis DRS analysis has shown that there is a shift in absorption edge as the dopant level increases. The energy band gaps of the ZnO NPs were estimated by using $E_g = 1239/\lambda_{\text{Edge}} \text{ eV}$. The absorption

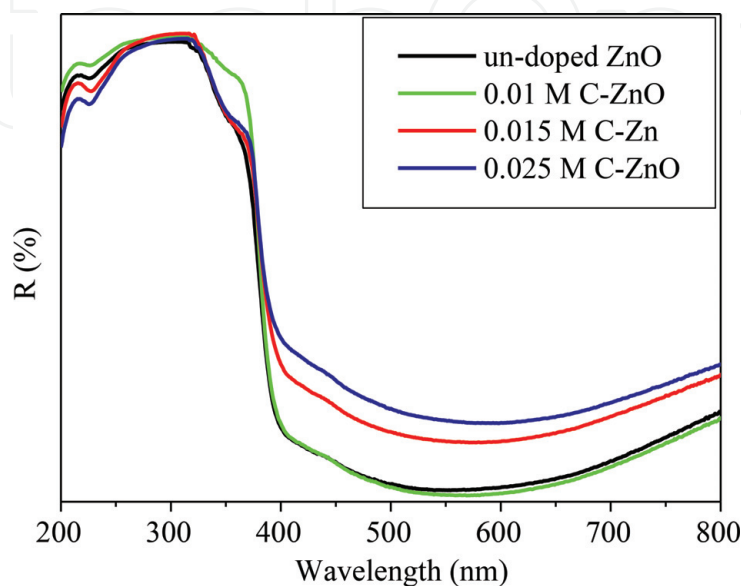


Figure 13.
The DRS spectra of the unmodified and C-ZnO samples synthesized by PSP system.

edge of the un-doped ZnO sample is 374 nm with an energy band gap 3.31 eV which is larger than for bulk ZnO NP with an absorption edge at 388 nm and energy band gap of 3.2 eV as revealed by the UV-Vis analysis. The absorption edges of the carbon-doped samples have revealed a red shift with energy band gaps of 3.29, 3.28 and 3.27 eV for the 0.01, 0.015 and 0.025 M of C-ZnO samples, respectively. This red shift in energy band gaps is probably due to size confinement effect.

8. Conclusion

Gathering knowledge about the challenges that other researchers experienced when working with spray pyrolysis for the production of ZnO together with understanding the properties and the crystal structure of ZnO has made it possible to design a novel pneumatic spray pyrolysis (PSP) system from ultrasonic spray pyrolysis (USP) for the deposition of ZnO NPs. The novel PSP system developed has presented unique features in material synthesis of ZnO nanostructures, like using the horizontal furnace reactor as compared to the vertical systems used in other techniques such as CVD, sol-gel, ion-assisted deposition etc. The horizontal system offers several advantages for thin film deposition in the absence of any tailing effect detected in the partial or oblique angle illustrations like in almost all the CVD methods. The samples in this system were deposited at 90° angle, which enables the aerosol beam comprised of the precursor solution vapor to directly cooperate with the substrate consistently. This system was able to produce the desired ZnO nanostructured properties for solar cell application. The SEM micrographs of both un-doped and carbon-doped samples have revealed the formation of spherical-shaped ZnO nanoparticles mesoporous morphology. The SEM images also revealed that the morphology and shape of the fabricated ZnO samples change as the dopant level increases. Additionally, the EDX analysis has confirmed the presence of Zn, C and O in the synthesized samples which indicates the successful pyrolysis of zinc ethoxide solution to form ZnO nanoparticles. The cross-sectional SEM has revealed the increase in film thickness as the dopant levels increase from 0.31 to 0.41 μm . The XRD has revealed the characteristic peaks of the hexagonal Wurtzite structure of ZnO for both un-doped and carbon-doped ZnO samples. XRD lines were observed at 31.90, 34.50, 36.34, 47.73, 56.88, 63.04, 68.20 and 77.33° and were indexed as (100), (002), (101), (102), (110), (103), (200) and (112), respectively. Additionally, the XRD analysis has also revealed a shift in the peaks to higher 2θ standards, which indicates the substitutional doping in the synthesized carbon-doped samples. Lastly, the UV-Vis DRS analysis has revealed a blue shift in absorption spectra of the synthesized samples with an increase in carbon doping.

Acknowledgements

The authors are grateful to the financial funding from their sponsors, the South African National Research Foundation (NRF), the Govan Mbeki Research and Development Centre (GMRDC) of the University of Fort Hare and the Sasol Inzalo Foundation. The authors would also like to acknowledge the DST/CSIR Nanotechnology Innovation Centre, National Centre for Nanostructured Materials, CSIR, and Centre of Image analysis and the University of Cape Town for the characterization of the ZnO NPs.

IntechOpen

Author details

Luyolo Ntozakhe^{1*} and Raymond Tichaona Taziwa²

1 Fort Hare Institute of Technology (FHIT), University of Fort Hare,
Republic of South Africa

2 Department of Applied Science, Walter Sisulu University (Postdam Campus),
East London, Republic of South Africa

*Address all correspondence to: Intozakhe@ufh.ac.za

IntechOpen

© 2019 The Author(s). Licensee IntechOpen. This chapter is distributed under the terms of the Creative Commons Attribution License (<http://creativecommons.org/licenses/by/3.0>), which permits unrestricted use, distribution, and reproduction in any medium, provided the original work is properly cited. 

References

- [1] Galstyan V, Comini E, Baratto C, Ponzoni A, Faglia G, Bontempi E. Growth and Gas Sensing Properties of Self-Assembled Chain-Like ZnO Nanostructures. *Process Engineering*. 2012;**47**:762-765
- [2] Banerjee AN. The design, fabrication, and photocatalytic utility of nanostructured semiconductors: Focus on TiO₂-based nanostructures. *Nanotechnology Science and Applications*. 2011;**4**:35-65
- [3] Zhou Q, Wen JZ, Zhao P, Anderson WA. Synthesis of Vertically-Aligned Zinc Oxide Nanowires and Their Application as a Photocatalyst. *Journal of Nanomaterials*. 2017;**7**:1-17
- [4] Zhang Y, Ram MK, Stefanakos EK, Goswami DY. Synthesis, Characterization, and Applications of ZnO Nanowires. *Journal of Nanomaterials*. 2012;**2012**:1-22
- [5] Cavallo C, Pascasio FD, Latini A, Bonomo M, Dini D. Nanostructured Semiconductor Materials for Dye-Sensitized Solar Cells. *Journal of Nanomaterials*. 2017;**2017**:1-31
- [6] Bhakat C, Singh PP. Zinc Oxide Nanorods: Synthesis and Its Applications in Solar Cell. *International Journal of Modern Engineering Research*. 2012;**2**:2452-2454
- [7] Aisah N, Gustiono D, Fauzia V, Sugihartono I, Nuryadi R. Synthesis and Enhanced Photocatalytic Activity of Ce-Doped Zinc Oxide Nanorods by Hydrothermal Method. *Materials Science and Engineering*. 2017;**172**:899-1757
- [8] Badreddine K, Kazah I, Rekaby M, Awad R. Structural, Morphological, Optical, and Room Temperature Magnetic Characterization on Pure and Sm-Doped ZnO Nanoparticles. *Journal of Nanomaterials*. 2018;**2018**:1-11
- [9] Zhang X, Qin J, Hao R, Wang L, Shen X, Yu R, et al. Carbon-Doped ZnO Nanostructures: Facile Synthesis and Visible Light Photocatalytic Applications. *Journal of Physical Chemistry C*. 2015;**119**:20544-20554
- [10] Nirmala M, Anukaliani A. Synthesis and characterization of undoped and TM (Co, Mn) doped ZnO nanoparticles. *Materials Letters*. 2011;**65**:2645-2648
- [11] Ozturk S, Kilinic N, Tsaltin N, Ozturk ZZ. Fabrication of ZnO nanowires and nanorods. *Physica E, Low-Dimensional Systems & Nanostructures*. 2012;**44**:1062-1065
- [12] Mah CF, Beh KP, Yam FK, Hassan Z. Rapid formation and evolution of anodized zn nanostructures in NaHCO₃ solution. *ECS Journal of Solid State Science and Technology*. 2016;**5**:105-112
- [13] Davinder R, Mukesh K, Sandeep KA. Deposition of nanocrystalline thin TiO₂ films for MOS capacitors using Sol-Gel spin method with Pt and Al top electrodes. *Solid State Electronics*. 2012;**76**:71-76
- [14] Zaleta-Alejandrea E, Camargo-Martinez J, Ramirez-Gariboa A, Pérez-Arrietab ML, Balderas-Xicohténcatla R, Rivera-Alvarez Z, et al. Structural, electrical and optical properties of indiumchloride doped ZnO films synthesized by Ultrasonic Spray Pyrolysis technique. *Thin Solid Films*. 2012;**524**:44-49
- [15] Yoo Y, Bruckenstein S. Synthesizing nanoparticles using reactions occurring in aerosol phases. *Advances in Nanoparticles*. 2013;**2**:313-317
- [16] Barthwal S, Kim YS, Lim SH. Fabrication of amphiphobic surface by using titanium anodization for large area three-dimensional substrates. *Journal of Colloid and Interface Science*. 2013;**400**:123-129

- [17] Jyotia M, Vijayb D, Radhac S. To Study the role of temperature and dodium hydroxide concentration in the synthesis of Zinc. *International Journal of Scientific Research Publications*. 2013;**3**:1-11
- [18] Bendavid A, Martin PJ, Preston EW. The effect of pulsed direct current substrate bias on the properties of titanium dioxide thin films deposited by filtered cathodic vacuum arc deposition. *Thin Solid Films*. 2008;**517**:494-499
- [19] Anders A, Lim S, Yu KM. High quality ZnO:Al transparent conducting oxide films synthesized by pulsed filtered cathodic arc deposition. *Thin Solid Films*. 2010;**518**:3313-3319
- [20] Baji Z, Labadia Z, Molnara G, Pecza B, Vad K, Horvatha ZE, et al. Highly conductive epitaxial ZnO layers deposited by atomic layer deposition. *Thin Solid Films*. 2014;**562**:485-489
- [21] Chun H, Takeshi S, Hiroyuki U, Yoshiki S, Naoto K. Fabrication of ZnO nanoparticles by pulsed laser ablation in aqueous media and pH-dependent particle size: An approach to study the mechanism of enhanced green photoluminescence. *Journal of Photochemistry and Photobiology A: Chemistry*. 2007;**191**:66-73
- [22] Foo KL, Kashif M, Hashim U, Ali ME. Fabrication and Characterization of ZnO Thin Films by Sol-Gel Spin Coating Method for the Determination of Phosphate Buffer Saline Concentration. *Current Nanoscience*. 2013;**9**
- [23] Kawabata K, Nanai Y, Kimura S, Okuno T. Fabrication of ZnO nanoparticles by laser ablation of sintered ZnO in aqueous solution. *Applied Physics A*. 2012;**107**:6745
- [24] Yuan X, Xua W, Huanga F, Cheng D, Wei Q. Polyester fabric coated with Ag/ZnO composite film by magnetron sputtering. *Applied Surface Science*. 2016;**390**:863
- [25] Kaushika VK, Mukherjeeb C, Gangulic T, Sena PK. Material characterizations of Al:ZnO thin films grown by aerosol assisted chemical vapour deposition. *Journal of Alloys and Compounds*. 2016;**689**:1028
- [26] Raghu P, Srinatha N, Naveen CS, Mahesh HM, Angadi B. Investigation on the effect of Al concentration on the structural, optical and electrical properties of spin coated Al:ZnO thin films. *Journal of Alloys and Compounds*. 2017;**68**:694
- [27] Rahman MA, Phillips MR. Ton-That C. Efficient multi-coloured Li-doped ZnO thin films fabricated by spray pyrolysis. *Journal of Alloys and Compounds*. 2017;**691**:339
- [28] Bagabas A, Alshammari A, Aboud MF, Kosslick H. Room-temperature synthesis of zinc oxide nanoparticles in different media and their application in cyanide photo-degradation. *Nanoscale Research Letters*. 2013;**8**:516
- [29] Mwakikunga BW. Progress in ultrasonic spray pyrolysis for condensed matter sciences developed from ultrasonic nebulization theories since michael faraday. *Critical Reviews in Solid State and Materials Sciences*. 2014;**39**:46-80
- [30] Taziwa R, Meyer E. Carbon Doped Nano-Crystalline TiO₂ Photo-Active Thin Film for Solid State Photochemical Solar Cells. *Advances in Nanoparticles*. 2014;**3**:54-63
- [31] Summary Related to Spray Freeze Dried Microspheres by means of an Ultrasonic Spray Nozzle. <https://microspray.com/spray-freeze-dried-microspheres-ultrasonic-spray-nozzle-7268112/>. [Accessed, 26 September 2018]
- [32] Ali A, Zafar H, Zia M, Haq I, Phull AR, Ali JS, et al. Synthesis,

characterization, applications, and challenges of iron oxide nanoparticles. *Nanotechnology. Science and Applications*. 2016;**9**:49-67

[33] Rajan R, Pandit AB. Correlations to predict droplet size in ultrasonic atomization. *Ultrasonics*. 2001;**39**:235-255

[34] Kurosawa M, Futami A, Higuchi T. Characteristics of liquids atomization using surface acoustic wave. *Mechanical Engineering*. 1997;**2**:801-804

[35] Dalmoro A, d'Amore M, Barba AA. Droplet size prediction in the production of drug delivery microsystems by ultrasonic atomization. *Translational Medicine @UniSa*. 2013;**7**:6-11

[36] Perednis D, Gauckler LJ. Thin Film Deposition Using Spray Pyrolysis. *Journal of Electroceramics*. 2005;**14**:103-111

[37] MateiGhimbeua C, Van Landschoot RC, Schoonman J, Lumbreras M. Preparation and characterization of SnO₂ and Cu-doped SnO₂ thin films using electrostatic spray deposition (ESD). *Journal of the European Ceramic Society*. 2007;**27**:207-213

[38] Suh WH, Suslick KS. Magnetic and porous nanospheres from ultrasonic spray pyrolysis. *Journal of the American Chemical Society*. 2005;**127**:12007-12010